Study of excited states in ^{85}Kr and ^{86}Kr: Evidence for neutron-core excitations in the N=50 nucleus ^{86}Kr

G. Winter, R. Schwengner, J. Reif, and H. Prade
Institut für Kern- und Hadronenphysik, Forschungszentrum Rossendorf, D-01314 Dresden, Germany

L. Funke
Ingenieurgesellschaft IAF Dresden, D-01326 Dresden, Germany

R. Wirowski, N. Nicolay, A. Dewald, and P. von Brentano
Institut für Kernphysik, Universität zu Köln, D-50937 Köln, Germany

H. Grawe and R. Schubart
Hahn-Meitner-Institut Berlin, D-14109 Berlin, Germany
(Received 30 April 1993)

High-spin states of the N=49,50 nuclei ^{85,86}Kr have been investigated via the reactions ^{82}Se(^{7}Li,$p3n$) or ^{82}Se(^{7}Li,$p2n$), respectively, using 32 MeV ^{7}Li ions. In order to suppress γ rays arising from pure neutron evaporation the measurements of angular distributions and relative excitation functions of the γ rays as well as $\gamma\gamma$ coincidences have been performed in particle-γ coincidence modes. Additional information on excited states in ^{85}Kr has been obtained in connection with the ^{82}Se(α,n) reaction at beam energies between 13 and 21 MeV. The level scheme of ^{85}Kr has been extended by a new sequence of high-spin states with excitation energies up to 4.8 MeV and tentative spins up to $(\frac{23}{2})$ that is built on top of the $\frac{17}{2}^+$ μs isomer at 1991.8 keV. For ^{86}Kr a new level scheme of high-spin states with excitation energies up to 7.9 MeV and tentative spins up to (12) has been observed for the first time. The level sequences observed in ^{85,86}Kr are interpreted on the basis of shell-model calculations in the configuration space $1p_{3/2}, 0f_{5/2}, 1p_{1/2}$, and $0g_{9/2}$ for the protons and $0g_{9/2}$ or $0g_{9/2}, 1d_{5/2}$ for the neutrons in ^{85}Kr or ^{86}Kr, respectively. The inclusion of neutron-core excitations in the calculations for ^{86}Kr results in a remarkably improved agreement between experimental and calculated level energies. In this way considerable contributions of neutron-core excitations are strongly suggested for the positive-parity yrast states with spins $7\hbar$, $9\hbar$, and $10\hbar$.

PACS number(s): 23.20.−g, 27.50.+e

I. INTRODUCTION

High-spin states in doubly even Kr nuclei reflect an almost complete variety of different modes of nuclear excitations. For light isotopes being close to the $N = Z$ line properties of strong quadrupole deformation and, at large angular momentum, of broken $0g_{9/2}$ proton and/or $0g_{9/2}$ neutron pairs have been identified (for recent experimental data see Ref. [1]). With increasing neutron number the $B(E2)$ values between levels of the yrast sequence decrease and few-particle excitations contribute more and more to the yrast states even at low spin. In ^{84}Kr that is only two neutrons apart from the magic number 50 two- and four-quasiparticle states play a dominant role in the yrast sequence [2]. Due to the absence of experimental data on high-spin states in ^{86}Kr it was not possible to trace which excitation modes appear or disappear when going to the nucleus with a closed neutron shell. Therefore an in-beam study of ^{86}Kr has been initiated. Excited states in ^{86}Kr have previously been studied in the radioactive decay of ^{86}Br, in Coulomb excitation, and in particle-transfer reaction experiments (see the recent compilation of Müller and Tepel [3]).

The excitation spectra of odd-mass Kr nuclei also exhibit quite different properties depending on the number of neutrons. This behavior is discussed in a similar way as for the doubly even nuclei. But, for odd-mass nuclei the polarization arising from the motion of both the unpaired neutron and broken pairs may also contribute to the formation of their shape, in particular for the soft nuclei close to ^{86}Kr. Thus, in ^{83}Kr that can be characterized by only three holes in the $N = 50$ shell the change from small deformation at low spin to strong prolate deformation for a positive-parity high-spin excitation is indicated [4]. In order to study the proton-neutron interaction and the influence of unpaired particles in the $N = 49$ nucleus a new in-beam study of ^{85}Kr has been carried out.

The most complete information available so far on the level scheme of ^{85}Kr originates from a previous (α,n) experiment [5]. This investigation revealed positive- and negative-parity states up to $E \approx 3$ MeV, but the highest spin observed was $I = \frac{13}{2}$.

In the course of a preceding in-beam investigation of ^{85,86}Kr based on irradiations of ^{82}Se targets with ^{7}Li ions Winter *et al.* [6] observed the isomeric behavior of the 4^+ yrast state in ^{86}Kr at 2250 keV and determined a half-life of that level of $T_{1/2}$= 3.1±0.6 ns. Furthermore, in that work a new iso-

meric $\frac{17}{2}^+$ state in ^{85}Kr at 1991 keV with a half-life of $T_{1/2} = (1.2^{+1.0}_{-0.4})$ μs was identified. Preliminary results on the level schemes of ^{85}Kr and ^{86}Kr as found in the present work have been published elsewhere [7, 8].

II. EXPERIMENTAL PROCEDURES AND RESULTS

Excited states in ^{86}Kr have been identified using in-beam γ-ray spectroscopy in connection with the ^{82}Se(^{7}Li,$p2n$) reaction at the cyclotron in Rossendorf and the FN-tandem accelerator in Cologne. Angular distributions of the γ-ray intensities and $\gamma\gamma$ coincidences have been measured during the bombardment of ^{82}Se foils (enrichment 92.2%) with 32 MeV ^{7}Li ions. In these experiments the cross section for producing Kr isotopes is only few percent of the total cross section since the probability for the emission of protons is rather small. In order to enhance γ rays arising from Kr isotopes in the measurements the particle-γ coincidence technique has been applied. Charged particles emitted during the irradiations have been detected by Si detectors of 100 μm effective thickness. Since in this thin layer the average energy loss of the emitted protons is considerably smaller than the energy loss of the emitted α particles, they can simply be distinguished by setting gates in the energy loss spectrum. In this way not only proton-γ coincidences at different observation angles but also proton-$\gamma\gamma$ coincidences have been measured. For this purpose 14 Si detectors have been mounted inside the OSIRIS-CUBE [9] at the Cologne FN-tandem accelerator and in connection with six Ge detectors proton-$\gamma\gamma$ and total $\gamma\gamma$ coincidences have been recorded. The arrangement of the Ge detectors in that spectrometer is also described in the paper by Schimmer *et al.* [10].

Excited states in ^{85}Kr have been studied in connection with the ^{82}Se(^{7}Li,$p3n$) reaction in the same experiment. Compared to ^{86}Kr the cross section for the population of states in ^{85}Kr is even smaller since the dominating part of the small proton-evaporation intensity flows in the (^{7}Li,$p2n$) reaction channel and forms ^{86}Kr.

In an attempt to enhance γ lines belonging to ^{85}Kr with respect to those belonging to ^{86}Kr we selected two adjacent proton gates in the energy loss spectrum [8]. The corresponding proton-$\gamma\gamma$ matrices contain about 9×10^6 and 7×10^6 true events, respectively, while 3×10^8 true events are collected in the total $\gamma\gamma$ matrix. Matrices of true events have been obtained by sorting the events containing time signals within and outside the peak of the time distribution in different matrices and subsequent subtraction.

Since the proton emission leading to the formation of ^{85}Kr is accompanied by an emission of three neutrons, while during the formation of ^{86}Kr only two neutrons are emitted, the kinetic energy of the protons belonging to ^{85}Kr should be somewhat smaller and, therefore, their energy loss somewhat larger than the corresponding quantities of ^{86}Kr. The intensity relations of some prominent γ-ray peaks in the projections of the total coincidence matrix and of the two proton-$\gamma\gamma$ matrices are illustrated in Fig. 1. The peaks dominating in the total matrix and belonging to pure neutron evaporation channels disappear completely in the proton-gated coincidences. The γ rays originating from excited states in ^{86}Kr are clearly enhanced in the matrix PROT1 gated by protons with lower energy loss while the γ rays belonging to ^{85}Kr are clearly enhanced if higher values for the energy loss are selected (matrix PROT2). In the lowest spectrum also γ rays belonging to other Kr isotopes are observed with considerable intensity (see caption to Fig. 1).

Some examples of background-corrected proton-$\gamma\gamma$ coincidence spectra derived from these two matrices are shown in Figs. 2 and 3. For the placement of γ rays with respect to the μs isomer in ^{85}Kr also delayed events from

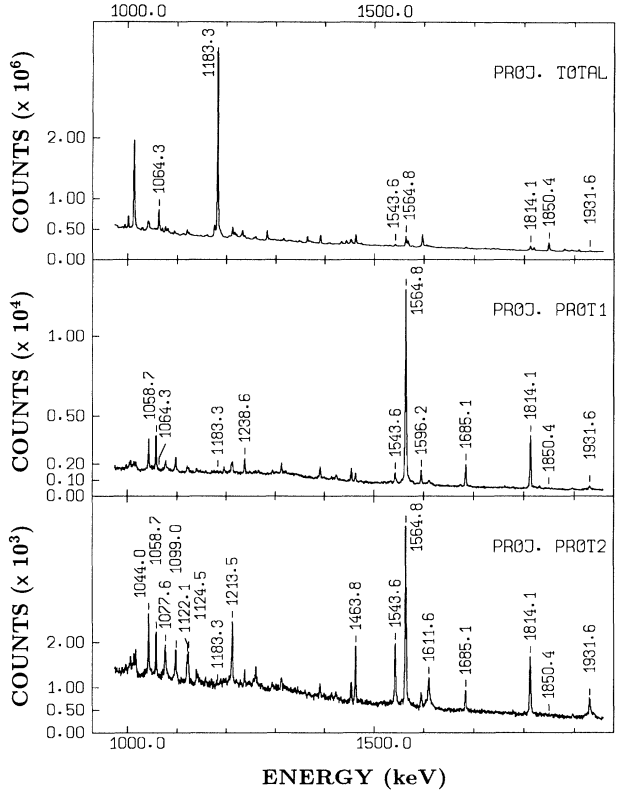

FIG. 1. Portions of the projections of the total $\gamma\gamma$ and of the two proton-$\gamma\gamma$ coincidence matrices. Random coincidences have been subtracted. The dominating peak at 1183.3 keV in the upper spectrum belongs to ^{85}Rb formed by pure neutron evaporation and vanishes in the projections of the proton-gated matrices PROT1 and PROT2. A similar behavior is found for the 1064.3 keV transition of ^{83}Br accompanied by emission of α particles. For the matrix PROT1 the selected value of the energy loss of the charged particles is somewhat smaller than for the matrix PROT2. Accordingly in the matrix PROT1 the γ rays connected with the $p2n$ reaction channel are enhanced with respect to the γ rays from the $p3n$ channel while the opposite situation is met in the matrix PROT2. Together with the lines of ^{85}Kr lines belonging to lighter Kr isotopes are also enhanced in the latter matrix. The lines at 1044.0 and 1099.0 keV arise from levels in ^{82}Kr, that at 1122.1 keV from ^{83}Kr, and those at 1077.6, 1124.5, 1213.5, and 1463.8 keV from ^{84}Kr.

the measurement of total $\gamma\gamma$ coincidences have been analyzed. For this purpose a time gate of 50 ns width was chosen outside the prompt peak of the time distribution. The spectrum of γ rays being in delayed coincidence with the 1931.6 keV transition in ^{85}Kr is shown in Fig. 4. In a separate proton-γ coincidence experiment the angular distributions of the γ-ray intensities have been measured (see Tables I and II).

Additional information on the spins of the levels in ^{85}Kr has been derived from a measurement of the relative excitation functions of the corresponding γ rays in the ^{82}Se(α, n) reaction using bombarding energies between 13 and 21 MeV (see Ref. [8]).

III. THE LEVEL SCHEMES

The information derived from the present experiments is summarized in level schemes for ^{85}Kr and ^{86}Kr. In the following subsections the main arguments for establishing these schemes are presented.

A. The level scheme of ^{85}Kr

The level scheme of ^{85}Kr found in the present in-beam study is shown in Fig. 5. The assignments of $\frac{11}{2}^+$ and $\frac{13}{2}^+$ to the levels at 1611.6 and 1931.6 keV, respectively, have been adopted from a previous (α, n) study [5]. In connection with irradiations of ^{82}Se targets with ^{7}Li ions

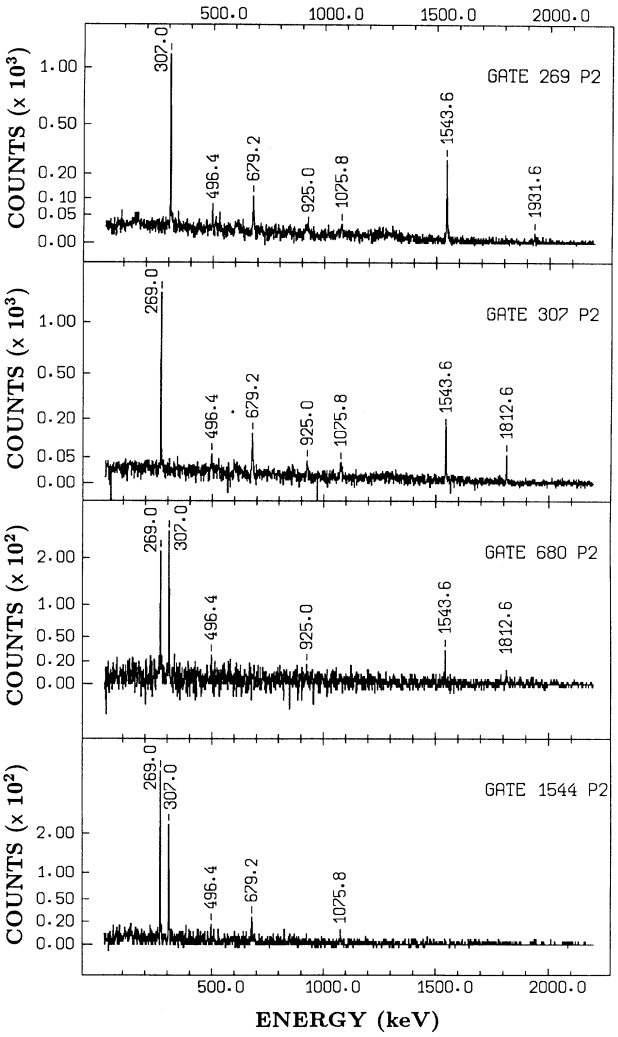

FIG. 2. Examples of proton-$\gamma\gamma$ coincidence spectra derived from the matrix PROT2 showing the new cascade in ^{85}Kr.

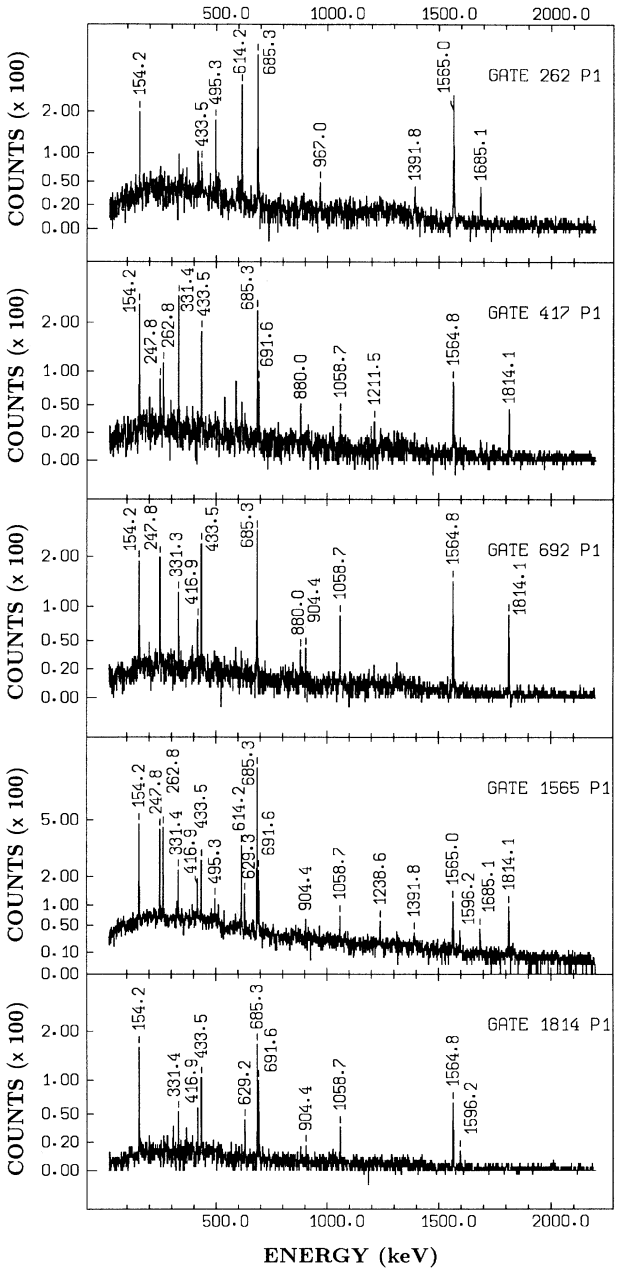

FIG. 3. Examples of proton-$\gamma\gamma$ coincidence spectra derived from the matrix PROT1 and used to deduce the new level scheme of ^{86}Kr.

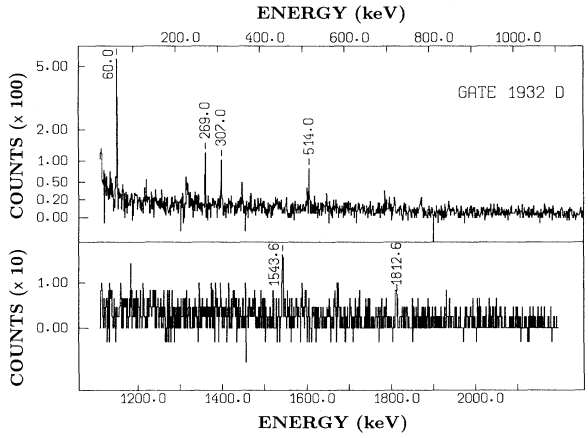

FIG. 4. Spectrum of delayed events derived from total $\gamma\gamma$ coincidences and gated by the 1931.6 keV transition in ^{85}Kr. The 60.0 keV line appears in this spectrum due to the broad distribution of time signals for that low-energy γ ray. The isomeric 514 keV transition of ^{85}Rb is caused by random coincidences.

the $\frac{17}{2}^+$ isomer at 1991.8 keV was established [6]. The spin and parity of that level have been derived [6] from measurements of both the internal conversion coefficient and the relative excitation function of the 60.2 keV γ ray.

Based on the results of prompt $\gamma\gamma$ coincidences a new cascade of four γ rays including the 1543.6 keV transition is established (see Fig. 2). This cascade is assigned to populate the $\frac{17}{2}^+$ μs isomer as derived from the spectrum of delayed $\gamma\gamma$ coincidences gated by the 1931.6 keV γ ray (see Fig. 4). The angular distribution of the 1543.6 keV γ ray points either to a stretched quadrupole transition or to a dipole transition between states of the same spin. The second possibility is preferred since in that case the spins of the new levels are $2\hbar$ smaller which is in agreement with the other observations. The 1812.6 keV transition then connects states differing in spin by $1\hbar$ while in the other case an $L = 3$ radiation must be assumed for the 1812.6 keV γ ray. (Unfortunately, the angular distribution of this γ ray could not be determined due to an overlap with a 1814.1 keV line of ^{86}Kr.) Furthermore, the relative excitation functions of the 1543.6, 269.0, and 307.0 keV γ rays in the (α, n) reaction [8] indicate that the spins of the corresponding levels are higher than $\frac{13}{2}$ the spin of the 1931.6 keV level. But the population of a state with a spin as high as $\frac{25}{2}$ (this value would be obtained for the observed state at 4111.4 keV if the 1543.6 keV transition is considered as a stretched quadrupole transition) in that experiment is very unlikely. Thus, tentative assignments of spins $\frac{17}{2}$, $\frac{19}{2}$, and $\frac{21}{2}$ to the levels at 3535.4, 3804.4, and 4111.4 keV, respectively, are preferred. Since a transition deexciting the new $\frac{17}{2}$ state at 3535.4 keV directly to the known $\frac{13}{2}^+$ state at 1931.6 keV was not observed we assign tentatively negative par-

TABLE I. Energies, intensities, and angular distribution coefficients for γ rays assigned to ^{85}Kr.

E_γ [a]	I_γ	A_2 [b]	A_4 [b]
60.2	12	-	-
269.0	24	-0.35(2)	-0.18(4)
307.0	27	-0.32(4)	-0.05(7)
319.9	2	-	-
342.4	≈1	-	-
679.2	8	-0.16(8)	-0.32(15)
1075.8	2	-	-
1261.3	≈2	-	-
1543.6	26	0.40(11)	-0.05(21)
1611.6	23	-0.28(7)	-0.03(12)
1812.6	13	- [c]	- [c]
1931.6	100	0.25(7)	-0.01(12)

[a]Gamma-ray energies are given in keV. The errors are between 0.1 and 0.4 keV.

[b]Coefficients deduced from γ-ray spectra measured at observation angles of 20°, 40°, 60°, and 90° in coincidence with outgoing protons.

[c]This value could not be determined due to the overlap with a 1814 keV line belonging to ^{86}Kr.

TABLE II. Energies, intensities, and angular distribution coefficients for γ rays assigned to ^{86}Kr.

E_γ [a]	I_γ	A_2 [b]	A_4 [b]
154.2	160	-0.19(3)	-0.05(5)
247.8	130	0.06(11)	-0.03(16)
262.8	125	-0.36(9)	-0.07(13)
325.3	40	-0.50(10)	0.4(2)
331.4	160	-0.35(3)	0.01(7)
416.9	110	-0.61(5)	-0.14(8)
433.5	200	-0.11(9)	0.05(13)
495.3	75	-0.14(10)	0.22(15)
614.2	180	-0.40(6)	-0.12(8)
629.3	95	-0.25(10)	0.01(19)
685.3	1000	0.30(5)	-0.10(8)
691.6	200	-0.33(6)	0.13(8)
758.2	≈40	-	-
880.0	≈50	-	-
904.4	50	-0.23(13)	0.27(19)
967.0	80	-0.5(2)	0.0(3)
1058.7	100	0.29(7)	-0.34(11)
1211.5	≈40	-	-
1238.6	50	0.5(2)	-0.6(2)
1313.7	35	-0.19(28)	-
1391.8	40	0.2(2)	-0.2(2)
1564.8	1100	0.46(9)[c]	-0.07(12)[c]
1566.3	≈350	-	-
1596.2	70	0.55(15)	-0.24(23)
1685.1	125	-0.40(10)	-0.21(13)
1814.1	340	0.23(7)[d]	-0.14(9)[d]

[a]Gamma-ray energies are given in keV. The errors are between 0.1 and 0.4 keV.

[b]Coefficients deduced from γ-ray spectra measured at observation angles of 20°, 40°, 60°, and 90° in coincidence with outgoing protons.

[c]This value is obtained for the doublet at 1565 keV.

[d]This value is influenced by a 1813 keV ΔI=1 transition (I_γ=150) belonging to ^{85}Kr.

ity to the levels of the new sequence of high-spin states.

Furthermore, according to our $\gamma\gamma$ coincidences the new $(\frac{17}{2}^-)$ level is connected to the $\frac{13}{2}^+$ level at 1931.6 keV via a cascade of the weak transitions at 342.4 and 1261.3 keV. In the spectrum of prompt $\gamma\gamma$ coincidences gated with the 1931.6 keV γ ray the intensity of the 1261.3 keV γ ray is somewhat larger than that of the 342.4 keV γ ray. Thus, the ordering of these two transitions in the cascade shown in Fig. 5 is indicated. A coincidence pair 1931-1262 keV was already observed in the previous (α, n) study [5] and $I^\pi = (\frac{11}{2}^+)$ was tentatively assigned to the corresponding level at 3193 keV. Due to the population of this level from the $(\frac{17}{2}^-)$ state we interpret, however, the measured angular distribution of the 1262 keV transition [5] as a $\Delta I = +1$ transition (instead of $\Delta I = -1$ [5]) and assign tentatively $I^\pi = (\frac{15}{2})$ to the 3193 keV state. Weak transitions at 496.4, 925.0, and 1075.8 keV have been assigned to ^{85}Kr (see Fig. 2) but a definite placement in the level scheme was not possible.

B. The level scheme of ^{86}Kr

The level scheme of ^{86}Kr deduced from the information of the present experiment is shown in Fig. 6. From previous work [3] the assignments of spin and parity $I^\pi = 2^+$ and 4^+ to the levels at 1565 and 2250 keV, respectively, were known. According to our $\gamma\gamma$ coincidences the 4^+ level is populated by γ rays at 1685.1, 1814.1, and 1566.3 keV. The values obtained for the angular distribution coefficients A_2 and A_4 (see Table II) point to a stretched quadrupole transition for the 1814.1 keV γ ray and to a $\Delta I = 1$ transition for the 1685.1 keV γ ray, respectively. We assign tentatively $I^\pi = (5^-)$ to the level at 3935.2 keV and negative parity also to the levels at 4430.5 keV (6^-) and 4693.4 keV (7^-). A (5^-) assignment to a level at 3935 keV was also derived [3] from (p, p') and (t, α) reaction data.

Spin and parity (6^+) are assigned to the level at 4064.2 keV that is deexcited by transitions at 247.8 and 1814.1 keV. The angular distribution of the 247.8 keV γ ray indicates a mixing of dipole and quadrupole components that leads us to propose a (5^+) assignment for the state at 3816.4 keV. From the coincidence data (Fig. 3) and the angular distributions the positive-parity sequence can be extended up to the (9^+) level at 5814.5 keV. For the higher-lying states the spin assignment is less certain since the angular distributions of the weak transitions at 880.0, 1211.5, and 1313.7 keV could not be determined since the first two of them overlap with lines in ^{84}Kr.

IV. SHELL-MODEL CALCULATIONS

Shell-model calculations for nuclei at or near to the $N = 50$ shell closure are usually carried out by considering ^{88}Sr as an inert core. For nuclei heavier than ^{88}Sr the proton orbitals $g_{9/2}$ and $p_{1/2}$ are most relevant and several nuclei of this region have carefully been analyzed in the shell model (see, e.g., Ref. [11]). For the Kr nuclei, however, the Fermi level in the proton system is

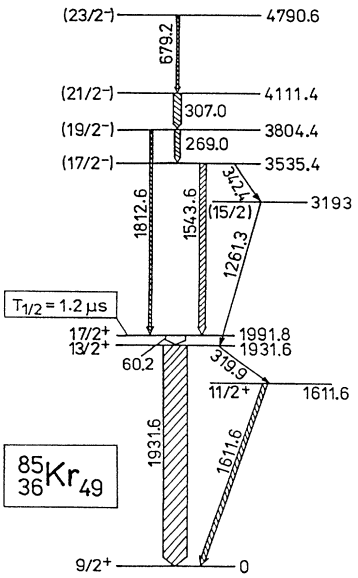

FIG. 5. Level scheme of ^{85}Kr as found in the present in-beam study. Low-spin states established in connection with the (α, n) reaction [5] are omitted.

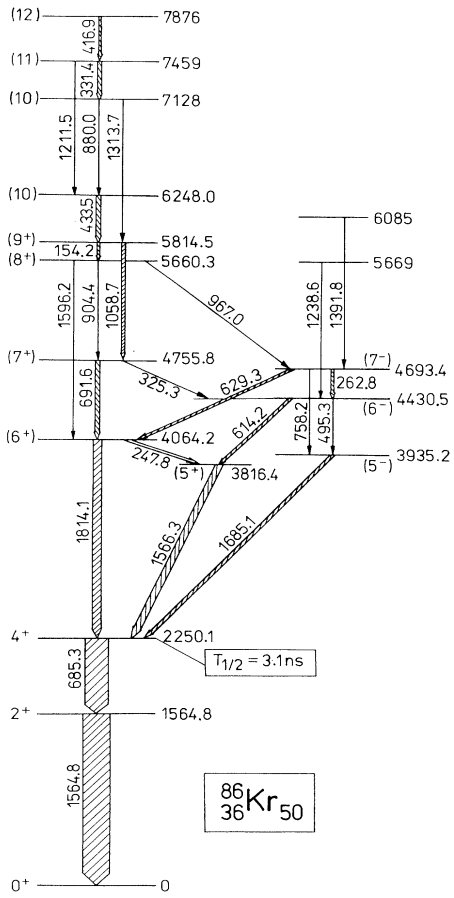

FIG. 6. Level scheme of ^{86}Kr deduced in the present in-beam study. Levels found in other experiments are compiled in Ref. [3].

close to the $1p_{3/2}$ or $0f_{5/2}$ orbitals and the high-j orbital $0g_{9/2}$ comes into play only at high excitation energies that are similar to the shell gap of the neutron system. Therefore, yrast configurations of high spin in ^{86}Kr might contain considerable contributions of particle-hole excitations of the closed neutron shell. In order to search for such core excitations shell-model calculations including neutron configurations have been carried out employing the code RITSSCHIL [12].

A. Residual interactions

The model space has been generated out of active $0f_{5/2}, 1p_{3/2}, 1p_{1/2}, 0g_{9/2}$ proton (π) and $0g_{9/2}, 1d_{5/2}$ neutron (ν) orbitals relative to a ^{68}Ni core. Since an empirical Hamiltonian for this configuration space is so far not available, it was necessary to combine different empirical Hamiltonians with results obtained from schematic nuclear interactions.

In a first schematic calculation of energy levels in ^{86}Kr only proton orbitals have been taken into account. The residual interactions have been approximated by two-body matrix elements of the surface delta interaction (SDI) [13] and single-particle energies with respect to a ^{78}Ni core have been taken from the paper of Ji and Wildenthal [14]. Since the influence of neutron-core excitations on the level energies of low-lying states is considered to be small, we adjusted the value of the strength parameter of the SDI and the single-particle energy of the $\pi 0g_{9/2}$ orbital in order to find a good description of the experimental energies up to 4.7 MeV. The value of the strength parameter obtained is $A_{T=1}$=0.35 MeV that is slightly larger than the recommended value $25A^{-1}$ MeV found from averaging over various mass regions [15]. The single-particle energy of the $\pi 0g_{9/2}$ orbital is mainly reflected in the average energy of the 5^-, 6^-, and 7^- states. These experimental energies are approximately reproduced for $\epsilon^{\pi}_{g_{9/2}} - \epsilon^{\pi}_{p_{3/2}}$= 2.912 MeV. The level energies obtained in this schematic calculation in a proton configuration space I (see Sec. IV B) are shown in the second column of Fig. 7.

Schematic calculations for ^{85}Kr including the neutron orbital $\nu 0g_{9/2}$ have shown that the experimental levels can be roughly reproduced when the $T = 0$ component of the proton-neutron interaction is calculated with the same value of the strength parameter as the proton-proton and neutron-neutron interaction ($A_{T=1} = A_{T=0}$= 0.35 MeV). The single-particle energy of the $\nu 0g_{9/2}$ orbital has been chosen in such a way that the difference between the experimentally known binding energies [16] of ^{85}Kr and ^{86}Kr was reproduced in the calculations.

In a second step we replaced various two-body matrix elements of the schematic calculation by empirically or experimentally determined values and included the neutron orbitals $\nu 0g_{9/2}$ or $\nu 0g_{9/2}$ and $\nu 1d_{5/2}$ in the calculations for ^{85}Kr or ^{86}Kr, respectively. The effective interaction in the proton shells has been taken from the paper by Ji and Wildenthal [14]. In that work the residual interaction and the single-particle energies of the proton orbitals are found in a least-squares fit to 170 experimental energy levels in $N = 50$ nuclei with mass numbers between 82 and 96. For the proton-neutron interaction connecting the $\pi(1p_{1/2}, 0g_{9/2})$ and the $\nu 0g_{9/2}$ orbitals the data given by Gross and Frenkel [17] have been used who derived the effective nuclear interaction in the $(1p_{1/2}, 0g_{9/2})$ space by an iterative fit to 95 experimentally known energies of states in N = 48, 49, and 50 nuclei. The matrix elements of the neutron-neutron interaction for the $0g_{9/2}$ orbital have been assumed to be equal to the $T = 1$ component of the $\pi\nu$ interaction given by Gross and Frenkel [17]. The diagonal matrix elements for the $\nu(0g_{9/2}, 1d_{5/2})$ multishell have been taken from the work of Li and Daehnick [18]. They determined the residual interaction by the particle-hole transformation of experimental energies of the multiplet $\nu(0g_{9/2}, 1d_{5/2})$ in ^{88}Sr. Following Muto *et al.* [19] we calculated the remaining matrix elements involving the $\nu 1d_{5/2}$ orbital with the SDI. Their values of the strength parameters [19], $A_{T=1}$=0.251 MeV and $A_{T=0}$=0.318 MeV, are somewhat smaller than the value found in our schematic calculation . For the $(\pi 0f_{5/2}, \nu 0g_{9/2})$ residual interaction the matrix elements proposed by Li *et al.* [20] have been applied.

The single-particle energies relative to the ^{68}Ni core have been derived from the single-particle energies of the proton orbitals given by Ji and Wildenthal [14] with respect to the ^{78}Ni core, from the neutron single-

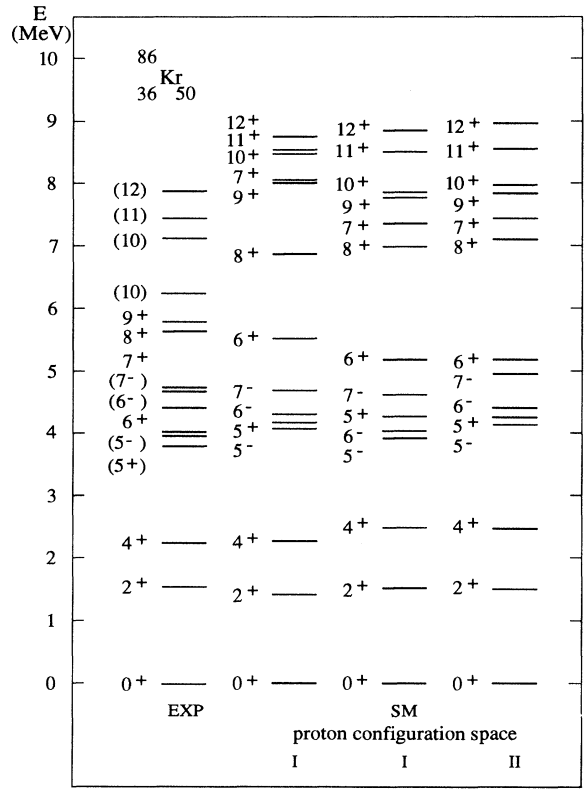

FIG. 7. Comparison of experimental and calculated level energies of ^{86}Kr for different assumptions on the configuration space for the protons. The level energies of the second column are obtained in the configuration space I but with a schematic residual interaction.

hole energy of the $0g_{9/2}$ orbital [17] and the neutron single-particle energy of the $1d_{5/2}$ shell [19] relative to the ^{88}Sr core. The transformation of these single-particle energies with respect to the ^{68}Ni core has been performed [11] on the basis of the effective residual interactions given before. The obtained values are, in MeV, $\epsilon^{\pi}_{f_{5/2}}=-9.806$, $\epsilon^{\pi}_{p_{3/2}}=-9.733$, $\epsilon^{\pi}_{p_{1/2}}=-3.023$, $\epsilon^{\pi}_{g_{9/2}}=-1.226$, $\epsilon^{\nu}_{g_{9/2}}=-6.583$, $\epsilon^{\nu}_{d_{5/2}}=-4.395$. Our final results for level energies and $E2$ transition probabilities in ^{85}Kr and ^{86}Kr are obtained by using these single-particle energies and the corresponding values for the strengths of the residual interactions.

The large energy separation between the $0f_{5/2}$ or $1p_{3/2}$ and the $0g_{9/2}$ proton orbitals arises from the parametrization of Ji and Wildenthal [14] that was carried out by an unrestricted adjustment of 35 parameters including both the energies of orbitals and the strengths of the residual interactions. Thus, mutual correlations between the energies and the interaction strengths might be suggested which result finally in a rather good description of the observed level energies of the proton system.

Very recently, a new parametrization of the interaction strength between proton orbitals in $N = 50$ nuclei has been performed [21] where the Kuo-Brown method [22] was applied to calculate the effective two-body interaction. Although a comparison [21] between these data and those of Ji and Wildenthal reveals marked deviations the level energies up to 5 MeV predicted by these two parametrizations for the proton system in ^{86}Kr are rather similar.

B. Configuration space

Due to the large number of active orbitals a truncation of the model space has been necessary to make the calculation feasible. For the calculation of states with $J \geq \frac{9}{2}$ in ^{85}Kr we adopted the assumption for $N = 49$ nuclei [23] that the energy levels up to 5 MeV can be described by coupling one neutron hole in the $0g_{9/2}$ orbital to the protons and the neutron $1d_{5/2}$ shell can be neglected. Considering the proton orbitals only it is sufficient to allow at most four protons to occupy the $0g_{9/2}$ shell while the occupation numbers of the other orbitals mentioned before have not been limited (proton configuration space I) [14]. The coupling of one neutron hole excitation in the $0g_{9/2}$ shell to this restricted proton space yields a model space which has dimensions of up to 10 000.

For the description of the high-spin states of ^{86}Kr the excitation of the $N = 50$ core must be included. It has been assumed that only one neutron is lifted from the $0g_{9/2}$ orbital over the shell gap to the $1d_{5/2}$ orbital. Since the coupling of this neutron particle-hole excitation to the proton configuration space I causes dimensions of the final space which cannot be handled with our computer further truncations of the model space for the protons have been necessary. A sufficient reduction of the rank of the Hamiltonian matrices to less than 19 000 can be achieved if not more than two protons are allowed to occupy the $0g_{9/2}$ orbital (proton configuration space II). The influence of the truncation of the proton space on the calculated level scheme of ^{86}Kr is demonstrated in Fig. 7, columns 3 and 4. For this illustration the neutron particle-hole excitations must be excluded. The restrictions in the model space for the protons lead to small changes in the positions of the positive-parity states, but to an increase of the energies for the negative-parity states by about 200–350 keV for levels below 5 MeV. The wave functions of these states are dominated by strong components contributing about 70% to the total final wave function and these components become somewhat more dominant when the dimension of the model space is reduced. The wave functions of the positive-parity high-spin states show a similar behavior.

V. RESULTS AND DISCUSSION

A. The nucleus ^{85}Kr

A comparison of experimental and calculated levels of ^{85}Kr is shown in Fig. 8. The calculation has been carried out in the large configuration space resulting from the coupling of one neutron hole in the $\nu 0g_{9/2}$ orbital to the proton configuration space I. The excitation energies of all experimentally known yrast states with $I^{\pi} \geq \frac{9}{2}^{+}$ or $I^{\pi} \geq \frac{15}{2}^{-}$ are well reproduced in the calculation. In particular, the small energy separation observed between the $\frac{13}{2}^{+}$ and $\frac{17}{2}^{+}$ yrast levels is also predicted by the shell model. An inspection of the wave functions reveals that the $\frac{11}{2}^{+}$, $\frac{13}{2}^{+}$ or $\frac{15}{2}^{+}$, $\frac{17}{2}^{+}$ states are predominantly formed by coupling the neutron hole to the lowest 2^{+} or 4^{+} states of the proton system, respectively. Similarly, the $\frac{15}{2}^{-}$, $\frac{17}{2}^{-}$ and $\frac{19}{2}^{-}$, $\frac{21}{2}^{-}$ states result mainly from the coupling of the neutron hole to the 5^{-} and 6^{-}

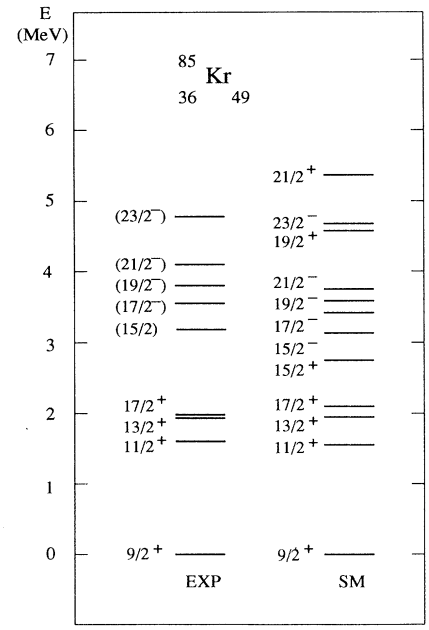

FIG. 8. Comparison of experimental and calculated level energies of ^{85}Kr. From the calculated levels only the yrast states with $I^{\pi} \geq \frac{9}{2}^{+}$ or $I^{\pi} \geq \frac{15}{2}^{-}$ are shown.

proton states, respectively. The lowest 7^- proton state dominates in the wave function of the $\frac{23}{2}^-$ level.

In ^{85}Kr two $B(E2)$ values between high-spin states are experimentally known ($\frac{17}{2}^+ \rightarrow \frac{13}{2}^+$ and $\frac{13}{2}^+ \rightarrow \frac{9}{2}^+$) that have been calculated using the wave functions found in the present analysis. For comparison these $B(E2)$ values have also been calculated using wave functions resulting from the parametrization of Sinatkas *et al.* [21] or from SDI (see Table III). The values of $B(E2, \frac{17}{2}^+ \rightarrow \frac{13}{2}^+)$ are found to deviate rather strongly from each other where the prediction based on the parametrization of Sinatkas *et al.* [21] agrees rather well with the experimental values. The other two calculations reflect the retardation of the $B(E2)$ value between the lowest 4^+ and 2^+ states in the proton system of ^{86}Kr discussed in the following subsection.

It should, however, be mentioned that the energies of the three yrast levels involved are also somewhat differently predicted in these three calculations. The energy separation between the $\frac{17}{2}^+$ and $\frac{13}{2}^+$ yrast states is markedly smaller [21] or larger (SDI) than found in the present calculation or in the experiment. The fair agreement between experimental and calculated level energies in ^{85}Kr might be considered as evidence for a proper description of the residual proton-neutron interaction that is also important for a reliable prediction of neutron-core excitations in the semimagic nucleus ^{86}Kr.

B. The nucleus ^{86}Kr

The final result of our calculation of level energies in ^{86}Kr is shown in Fig. 9 together with the experimentally observed levels (see column 1). When comparing the level energies resulting from the calculation in the pure proton configuration space II (column 3) and in the configuration space extended by neutron-core excitations (column 2), respectively, a drastic reduction of some yrast energies becomes evident. Whereas the 2^+, 4^+, and 5^+ yrast states as well as the 5^-, 6^-, and 7^- levels are only very weakly shifted by including the $\nu(g^9_{9/2}, d^1_{5/2})$ configuration, shifts as much as 2.2, 1.5, and 1.3 MeV are obtained for the 7^+, 9^+, and 10^+ yrast levels, respectively. Up to the experimentally observed I=(10) yrast state at 6248.0 keV our experimental observations are in good agreement with this strongly altered sequence of calculated excitation energies.

For the states observed at higher excitation energies a parity assignment was not possible. Thus, these states might be compared with calculated levels of either positive or negative parity. Levels with spins between $10\hbar$ and $12\hbar$ are predicted in this energy region for both parities. It should be mentioned that their energies are also strongly affected by the inclusion of neutron-core excitations.

The general agreement between observed and calculated level energies is interpreted as a clear indication for the presence of particle-hole excitations of the closed neutron core in some of the yrast states of positive parity in ^{86}Kr. The influence of the neutron particle-hole excitations for yrast states is also reflected in some of the wave functions obtained in the calculations for states at high excitation energies. The states of positive parity below 4 MeV and the negative-parity states with spins up to 9^- are dominated by proton configurations. For the 4^+ yrast level at 2250.1 keV the configuration $(f^5_{5/2}, p^3_{3/2})$ is predicted as the main component which is in agreement with experimental data from particle-transfer reactions [3].

The half-life of this level, $T_{1/2}$ = 3.1± 0.6 ns, determined in the course of a preceding investigation [6], implies a very small $B(E2)$ value for the transition to the 2^+ yrast state (for a discussion see Ref. [6]). This $B(E2)$ value as well as that between the 2^+ yrast state and the 0^+ ground state have been calculated within the shell model using wave functions belonging to different parametrizations of the residual interaction (see Table III). In this comparison neutron particle-hole excitations have been neglected. The strong retardation

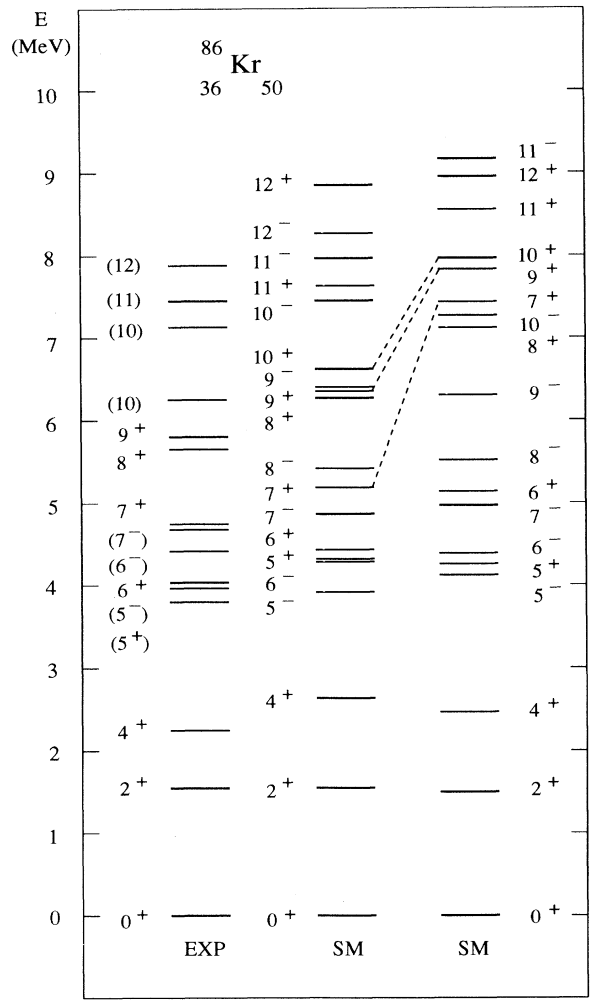

FIG. 9. Influence of neutron-core excitations on the calculated level energies of ^{86}Kr. From the calculated levels only the yrast states of positive parity (except the 1^+ and 3^+ states) and the yrast states of negative parity with $I^\pi \geq 5^-$ are shown.

TABLE III. $B(E2)$ values in ^{85}Kr and ^{86}Kr.

Nucleus	$I_i \rightarrow I_f$	$B(E2)_{\text{expt}}$ [a]	$B(E2)_{\text{calc.}}$ [a,b]	$B(E2)_{\text{calc.}}$ [a,c]	$B(E2)_{\text{calc.}}$ [a,d]
^{85}Kr	$\frac{13}{2}^+ \rightarrow \frac{9}{2}^+$	$2.8\ ^{+0.4}_{-0.3}$ [e]	2.1	6.4	2.1
	$\frac{17}{2}^+ \rightarrow \frac{13}{2}^+$	$3.8\ ^{+1.8}_{-1.8}$	0.56	3.4	0.01
^{86}Kr	$2^+ \rightarrow 0^+$	$10.8^{+0.9}_{-0.9}$ [f]	4.2	6.2	4.1
	$4^+ \rightarrow 2^+$	$0.054\ ^{+0.013}_{-0.009}$	0.58	0.003	0.10

[a] $B(E2)$ values are given in Weisskopf units (22.5 e^2 fm^4). In the calculations effective charges [24] of 1.35e and 0.35e have been used for protons and neutrons, respectively.
[b] Wave functions obtained in the present work.
[c] Wave functions of Sinatkas *et al.* [21].
[d] SDI wave functions (see text).
[e] Reference [5].
[f] Reference [25].

of the $B(E2)$ value between the 4^+ and 2^+ yrast states is rather well reproduced using the parametrizations of Sinatkas *et al.* [21] or SDI while the wave functions based on the residual interaction of Ji and Wildenthal [14] predict only a moderate reduction of that B(E2) value.

Using the Ji-Wildenthal interaction [14], significant components containing the neutron cluster $\nu(g^9_{9/2}, d^1_{5/2})_J$ are obtained for the positive-parity states above 4.5 MeV where the neutron angular momentum J takes the values $5\hbar$, $6\hbar$, and $7\ \hbar$. Dominating contributions to the lowest 5^+, 6^+, and 7^+ states result from coupling this neutron cluster to the proton excitation 0^+. The lowest 8^+ state is mainly formed from the neutron cluster with $J = 6\hbar$ and the 2^+ proton excitation while the lowest 9^+, 10^+, and 11^+ states arise from an aligned coupling of the neutron cluster to the 4^+ proton excitation. It should be noted here that the excitation energy of the I=8^+ level can be well reproduced as a $\pi(0g^2_{9/2})_{8+}$ configuration with the interaction of Sinatkas *et al.* [21].

VI. SUMMARY

The results of an in-beam study of high-spin states of ^{85}Kr and ^{86}Kr via the reactions ^{82}Se(^{7}Li,$p3n$)^{85}Kr and ^{82}Se(^{7}Li,$p2n$)^{86}Kr, respectively, are presented. For ^{85}Kr also data derived in connection with the (α, n) reaction are involved. In ^{85}Kr a new sequence of high-spin states has been established on top of the $\frac{17}{2}^+$ μs isomer. A completely new level scheme of high-spin states in ^{86}Kr extending up to 7.9 MeV and I= (12) has been deduced. Shell-model calculations have been carried out to interpret these experimental results. The high-spin states in ^{85}Kr extending up to an I=($\frac{23}{2}^-$) state at 4.8 MeV can be well described by coupling one neutron hole in the $\nu 0g_{9/2}$ shell to the excitations of the proton system. For the $N = 50$ nucleus ^{86}Kr one-particle–one-hole excitations of the closed neutron shell have been taken into account. As a result of this analysis the positive-parity yrast states with $I^\pi \geq 6^+$ contain considerable admixtures of neutron-core excitations that even seem to dominate in the yrast states with $I^\pi = 7^+$, 9^+, and 10^+. The strong retardation of the $B(E2)$ value for the transition between the 4^+ and 2^+ yrast states is well described by shell-model wave functions.

ACKNOWLEDGMENTS

This work was supported by the Deutsche Forschungsgemeinschaft (DFG) under Contract Nos. Fu 238/1-1, Br 799/5-1, and Wi 1230/1-1 and by the Bundesministerium für Forschung und Technologie under Contract No. 06DR103.

[1] J. Heese, D.J. Blumenthal, A.A. Chishti, P. Chodhury, B. Crowell, P.J. Ennis, C.J. Lister, and Ch. Winter, Phys. Rev. C **43**, R921 (1991).
[2] H. Rotter, J. Döring, L. Funke, L. Käubler, H. Prade, R. Schwengner, G. Winter, A.E. Zobov, A.P. Ginberg, I.Kh. Lemberg, A.S. Mischin, L.A. Rassadin, I.N. Chugunov, A.D. Efimov, K.I. Erokhina, V.I. Isakov, L.O. Norlin, and U. Rosengard, Nucl. Phys. **A514**, 401 (1990).
[3] H.W. Müller and J.W. Tepel, Nucl. Data Sheets **54**, 527 (1988).
[4] P. Kemnitz, J. Döring, L. Funke, G. Winter, L.H. Hildingsson, D. Jerrestam, A. Johnson, and Th. Lindblad, Nucl. Phys. **A456**, 89 (1986).
[5] A.E. Sobov, Ph.D. thesis, Leningrad State University, 1986 and Contributed papers 36; *Proceedings of the Conference on Nuclear Spectroscopy and Nuclear Theory,* Kharkov, USSR, 1986 (Nauka, Leningrad, 1986), pp. 72–74.
[6] G. Winter, J. Döring, L. Funke, L. Käubler, R. Schwengner, and H. Prade, Z. Phys. A **332**, 33 (1989).
[7] G. Winter, L. Funke, R. Schwengner, H. Prade, R. Wirowski, N. Nicolay, A. Dewald, and P. von Brentano, Z. Phys. A **343**, 369 (1992).
[8] G. Winter, L. Funke, R. Schwengner, H. Prade, R. Wirowski, N. Nicolay, A. Dewald, and P. von Brentano, Z. Phys. A **344**, 229 (1992).

[9] R. Wirowski, Ph.D. dissertation, Universität zu Köln, 1993.
[10] M. Schimmer, S. Albers, A. Dewald, A. Gelberg, R. Wirowski, and P. von Brentano, Nucl. Phys. **A539**, 527 (1992).
[11] J. Blomqvist and R. Rydström, Phys. Scr. **31**, 31 (1985).
[12] D. Zwarts, Comput. Phys. Commun. **38**, 365 (1985).
[13] P.W.M. Glaudemans, P.J. Brussaard, and B.H. Wildenthal, Nucl. Phys. **A102**, 593 (1967).
[14] X. Ji and B.H. Wildenthal, Phys. Rev. C **37**, 1256 (1988).
[15] P.J. Brussaard and P.W.M. Glaudemans, *Shell-Model Applications in Nuclear Spectroscopy* (North-Holland, Amsterdam, 1977).
[16] A.H. Wapstra and G. Audi, Nucl. Phys. **A432**, 1 (1985).
[17] R. Gross and A. Frenkel, Nucl. Phys. **A267**, 85 (1976).
[18] P.C. Li and W.W. Daehnick, Nucl. Phys. **A462**, 26 (1987).
[19] K. Muto, T. Shimano, and H. Horie, Phys. Lett. **135B**, 349 (1984).
[20] P.C. Li, W.W. Daehnick, S.K. Saha, J.D. Brown, and R.T. Kouzes, Nucl. Phys. **A469**, 393 (1987).
[21] J. Sinatkas, L.D. Skouras, D. Strottman, and J.D. Vergados, J. Phys. G **18**, 1377 (1992).
[22] T.T.S. Kuo and G.E. Brown, Nucl. Phys. **85**, 40 (1966); **A114**, 241 (1968).
[23] R. Gross and A. Frenkel, Phys. Lett. **53B**, 227 (1974).
[24] M.K. Kabadiyski, F. Cristancho, C.J. Gross, A. Jungclaus, K.P. Lieb, D. Rudolph, H. Grawe, J. Heese, K.-H. Maier, J. Eberth, S. Skoda, W.-T. Chou, and E.K. Warburton, Z. Phys. A **343**, 165 (1992).
[25] S. Raman, C.H. Malarkey, W.T Milner, C.W. Nestor, and P.H. Stelson, At. Data Nucl. Data Tables **36**, 1 (1987).